HYFI: Hybrid Floor Identification Based on Wireless Fingerprinting and Barometric Pressure

Fang Zhao, Haiyong Luo, *Member, IEEE*, Xuqiang Zhao, Zhibo Pang, *Senior Member, IEEE*, and Hyuncheol Park

***Abstract*—Identifying different floors in multistory buildings is a very important task for precise indoor localization in industrial and commercial applications. The accuracy from existing studies is rather low, especially in multistory buildings with irregular structures such as hollow areas, which is common in various industrial and commercial sites. As a better solution, this paper proposes a hybrid floor identification (HYFI) algorithm, which exploits wireless access point (AP) distribution and barometric pressure information. It first extracts the distribution probability of APs scanned in different floors from offline training fingerprints and adopts Bayesian classification to accurately identify floor in well-partitioned zones without hollow areas. The floor information obtained from wireless AP distribution is then used to initialize and calibrate barometric pressure-based floor identification to compensate variable environmental effects. Extensive experiments confirm that the HYFI approach significantly outperforms purely wireless fingerprinting-based or purely barometric pressure-based floor identification approaches. In our field tests in multistory facilities with irregular hollow areas, it can identify the floor level with more than 96.1% accuracy.**

***Index Terms*—Barometric pressure, floor identification, hybrid, indoor positioning, wireless fingerprinting.**

I. Introduction

ACCURATE and real-time indoor localization has become an increasing demand for in-building navigation, asset and personnel tracking, message delivery, emergency support, etc. in industrial applications such as mining automation [1], robot system [2], industrial automation [3], autonomous vehicle [4], and construction safety [5]. Although numerous research works on indoor positioning with wireless networks have been conducted, accurate floor identification remains a big challenge. For modern industrial and commercial buildings, there exist many complex and irregular inner structures, such as hollow areas through multiple floors. In this case, the received signal strength (RSS)-based localization algorithm (e.g., fingerprinting positioning) cannot accurately identify which floor the targets are situated on when they are moving around the hollow interior zone due to small wireless signal propagation attenuation between adjacent floors.

In multistory buildings, floor identification can be used to reduce space search domain and improve localization accuracy. In emergency situations, the accurate floor information is critical for rescuers or rescue robots to promptly obtain the victims' floor information to provide effective and efficient emergency services [6]. The floor information on which the moving objects are situated can be used to improve the effectiveness of message delivery.

With proliferation of barometric sensors embedded in smartphones (e.g., xiaomi2/3/4/5, Samsung S4/Note2/3/4, and iphone6), employing altitude deducing from barometric pressure to identify floor level becomes an alternative method. However, due to the device heterogeneity and weather change, barometric pressure measurements cannot be used to identify floor level directly without calibration. In order to mitigate the inconsistence and instability of pressure measurements, most existing methods employ a standard barometer deployed in the target building to calibrate the barometric sensors embedded in smartphones. These methods require deploying additional barometric infrastructure and communicating with the calibration center frequently with heavy power consumption.

Different from the above-mentioned floor identification methods, we propose a novel hybrid floor identification (HYFI) algorithm, which exploits wireless access point (AP) distribution and barometric pressure information together. It first extracts the distribution probability of all APs sensible on each floor in a multistory building with the offline training fingerprints, and then adopts Bayesian classification to accurately identify floor level in the well-partitioned zones without hollow areas. The high-reliable floor information obtained from AP distribution is then used to calibrate barometric sensor for accurate floor identification on those easily confused floors with hollow areas. The proposed algorithm leverages the existing Wi-Fi networks without the need of deploying a standard barometer in the building. It is lightweight and can be run on the commodity smartphones.

Manuscript received February 11, 2015; revised May 02, 2015 and August 31, 2015; accepted October 03, 2015. Date of publication October 16, 2015; date of current version February 06, 2017. This work was supported in part by the National Natural Science Foundation of China under Grant 61374214, in part by the 863 Achievement Transformation Project of Tianjin under Grant 14RCHZGX00857, and in part by the Open Project of the Beijing Key Laboratory of Mobile Computing and Pervasive Device. Paper no. TII-15-0256.

F. Zhao is with the School of Software Engineering, Beijing University of Posts and Telecommunications, 100083 Beijing, China.

H. Luo is with the Institute of Computing Technology, Chinese Academy of Sciences, 100190 Beijing, China.

X. Zhao is with the School of Computer Science and Technology, Beijing Institute of Technology, 100081 Beijing, China.

Z. Pang is with Corporate Research, ABB AB, 72178, Västerås, Västmanland, Sweden.

H. Park is with the Samsung Electronics Corporation, Suwon-si, Gyeonggi-do 16677, South Korea.

Color versions of one or more of the figures in this paper are available online at http://ieeexplore.ieee.org.

Digital Object Identifier 10.1109/TII.2015.2491264

This paper is organized as follows. In Section II, the related work is presented. The Bayesian classification-based floor identification algorithm is described in Section III. The pressure-based floor identification algorithm is introduced in Section IV. The hybrid floor-level identification algorithm based on AP distribution feature and barometric pressure is proposed in Section V. Finally, the conclusion of this paper is made in Section VI.

II. Related Work

In recent years, there are many indoor localization techniques for personnel, asset tracking, and robot navigation, such as Wi-Fi [7], ZigBee [8], ultrasonic sensors [9], vision [10], laser [11], and inertial sensor [12]. These techniques can deliver good localization accuracy, but need to deploy special infrastructure except for Wi-Fi and inertial sensor. The Wi-Fi fingerprinting positioning directly explores the prevalent wireless network and becomes the most widespread approach for indoor localization.

However, the rather low accuracy of Wi-Fi localization (e.g., 3–10 m) is not adequate for accurate floor localization in the multistory buildings with complex and irregular structure, such as hollow interior, which is very popular in modern super malls and industrial facilities. In the well-partitioned tall buildings, because adjacent floors are partitioned with heavy concrete floor slabs, the RSS difference between different floors is large due to heavy concrete floor slabs between adjacent floors. Therefore, the floors can be accurately discriminated. However, in the complex industrial environments, there are many irregular structures, such as hollow interior and, thin floor slab, the rather low vertical accuracy of Wi-Fi localization cannot accurately discriminate adjacent floors due to signal variation and small signal propagation attenuation between adjacent floors. Therefore, in complex and irregular multistory industrial environments, the floor determination is a big challenge and needs to be handled to extend the capability of indoor positioning system.

Some work has been done for floor identification. Skyloc [13] employs Global System for Mobile Communications (GSM) signal strength fingerprint to identify floor with K-Nearest Neighbors (KNN) algorithm (K-nearest neighbors with shortest Euclidean distance) and obtains 73% accuracy. The Group Variance algorithm [14] groups Wi-Fi Received Signal Strength Index (RSSI) associating with each floor and identifies the floor level based on the best match of group variance. Deng *et al.* used k-means clustering algorithm to identify floor [15]. The accuracy is limited and cannot discriminate the floors with complex and irregular structure.

As an alternative method, barometric altimetry is used for floor determination. From the observation that absolute pressure readings have significant time-of-day variations, and the pressure difference across different floor pairs keeps consistent, Muralidharan *et al.* used pressure difference as a fingerprint to detect exact number of floors changed and vertical activities (e.g., taking escalators, stairs, or elevators) with almost 100% accuracy [16]. However, it is difficult to directly use the barometer to determine the actual floor. To tackle barometric variation with temperature and environmental changes in a fixed place, Liu *et al.* introduced a floor determination approach based on differential barometric altimetry [17]. By deploying barometer in the base station as reference, it gets accurate altitude from filtering and calculating the atmospheric pressure measured by base station and mobile station simultaneously with about 1.0-m relative accuracy.

To avoid deploying barometer infrastructure, Ye *et al.* presented a floor localization method based on mobile phone sensing [18]. By capturing user encounters and analyzing user trails, the algorithm first constructs a mapping from the traveling time (in elevator) or the step counts (walking on the stairs) between any two floors to the number of floor levels, and then use the mapping to pinpoint floor levels. Because the accelerometer sensor is susceptible to various perturbations, the accuracy of floor localization only with accelerometer in multistory building is limited. Furthermore, the algorithm requires the user to input ground-truth floor when encountering others on a floor level or in the elevator), which is inconvenient and limits its practical application. Another floor localization system [19] recently designed by Ye *et al.* uses the barometer on smartphone only and builds the barometer fingerprint map which contains the barometric pressure value for each floor level with crowdsourcing to locate users' floor. It does not rely on Wi-Fi infrastructure and requires neither war-driving nor prior knowledge of the buildings. However, it takes rather long time to calibrate the barometric sensor using opportunistic encounter in the same elevator and the system converges slowly before providing accurate floor identification service.

III. Bayesian Classification-Based Floor Identification Algorithm

In this section, a Bayesian Classification-Based Floor Identification Algorithm (hereinafter referred to as BCFI) is proposed, which treats the floor identification as a probability estimation problem. It first obtains the prior probability of all APs with Wi-Fi-enabled devices on each floor in a multistory building in the training phase, and then calculates the posterior probability that the target is situated on each floor with the latest signal observation. Compared with the methods based on the traditional shortest distance criteria, this probability-based method can achieve more floor identification accuracy.

A. Fundamental of Floor Identification Using Wi-Fi Signal

In multistory buildings, Wi-Fi signal is attenuated by about 0.342 to 0.36 dB/cm through an interior wall or a partition, and about 0.577 to 0.699 dB/cm through a concrete wall [20]. When a Wi-Fi signal propagates through a floor made of mat reinforcement concrete, the signal will result in a sudden and remarkable attenuation (e.g., 50-cm-thick concrete causes about 29-dB attenuation). On the other hand, when the signal propagates on the same floor, the path attenuation is stable (i.e., proportional to the propagation distance and the number of crossing room partition walls made of brick concrete). The propagation attenuation patterns within a multistory building result in differentiable AP set and associated sensible probabilities that devices receive on different floors, which can be used as the specific floor fingerprints (AP set and corresponding sensible probabilities) for floor identification.

B. BCFI Algorithm

The BCFI algorithm adopts Bayesian estimation to calculate the probability on which floor a user is located using the above-described floor fingerprint. The floor with the largest posterior probability is taken as the final floor estimation.

The BCFI algorithm consists of two stages. In the first stage (offline training stage), we first uses Wi-Fi-enabled devices (e.g., smartphones) to scan access points (APs) in a building to collect training fingerprints, and then perform statistical analysis to obtain the sensible probability of each AP on different floors on a server. In the second stage (online floor identification stage), when a new Wi-Fi fingerprinting is obtained, the probability is calculated using Bayesian estimation [21]. Because the calculation cost is lightweight, the online floor identification can be run on each smartphone in a distributed and scalable way.

For the convenience of description, let $L = \{l_1, l_2, \ldots, l_n\}$ represent the n consecutive floors of a multistory building. Assuming that there are p APs that can be scanned (sensible) in the building and let $Z = \{Z_1, Z_2, \ldots, Z_p\}$, where Z_i denotes the ith sensible AP. $O = \{o_1, o_2, \ldots, o_k\}$ is the set that consists of k observations, where $o_j = (z_1, z_2, \ldots, z_m)$ $(z_k \in Z)$ indicates an observation consisting of m APs. Considering the fact that the number of scanned APs in different locations on a floor is different, the dimension of observation vector $o_j = (z_1, z_2, \ldots, z_m)$ is dynamic. A two-tuple (o_j, l_p) $(\mathrm{o_j} \in \mathrm{O},\ l_p \in L)$ is introduced to represent the training and testing samples.

Refer to (1), the posteriori probability distribution $P(l_p|o_j)$ of the target floor is proportional to the product of prior probability $P(l_p)$ and the likelihood function $P(o_j|l_p)$. The likelihood function $P(o_j|l_p)$ is the probability corresponding to the observation $o_j = (z_1, z_2, \ldots, z_m)$ on the condition that the target is located on the pth floor. The prior probability $P(l_p)$ shows floor uncertainty before online observation is considered. It is related to users' behavior and can be obtained by the statistical analysis of massive observations

$$\mathrm{P}(l_p|\mathrm{o}_j) = \frac{P(o_j|l_p)P(l_p)}{\sum_{p=1}^{n} P(o_j|l_p)P(l_p)} \propto P(o_j|l_p)P(l_p). \quad (1)$$

It is nontrial to obtain the prior probability from massive users' daily behaviors. As a simplified alternative, we obtain the prior probability distribution $P(l_p)$ from the offline training samples, i.e., $P(l_p)$ is the sample number collected on the pth floor over the total sample number collected on all floors in a building. By this way, the prior probability on different floors will be similar if the path lengths for training data collection on different floors are approximate. This training sample-based prior probability is artificial. If we want to get an accurate prior probability, the floor distribution of training samples should keep in line with the pattern of users' daily lives.

Assuming that all APs are independent, the likelihood function $P(o_j|l_p)$ is the product of the probabilities of all sensible APs in the observed data $o_j = (z_1, z_2, \ldots, z_m)$ $(z_k \in Z)$, as the formula (2) states. $P(z_k|l_p)$ is the probability that the AP z_k can be scanned on the floor l_p, i.e., the probability $P(z_k|l_p)$ is the number of training samples including the AP z_k divided by the total number of training samples collected on the l_p floor

$$P(\mathrm{o}_j|\mathrm{l}_p) = \prod_{k=1}^{m} P(z_k|l_p). \quad (2)$$

Once an observation is obtained, the posterior probability $P(l_p|o_j)$ on each floor is calculated with the above-mentioned prior probability $P(l_p)$ and likelihood function $P(o_j|l_p)$ equation. We choose the floor with the largest posterior probability as the final floor estimate.

C. Algorithm Complexity Analysis

The main operation of BCFI is to perform statistical analysis of training samples in offline phase on a server. Corresponding computation complexity is $O(m * k)$, where k is the total sample number and m is the whole scanned AP number in a sample. In the online floor identification phase, the main task is to calculate the likelihood value $P(o_j|l_p)$. The calculation complexity of $P(o_j|l_p)$ is $O(n * m)$, where n is the floor number and m is the AP number in a sample. In real application, the parameters n (floor number) and m (AP number) are small. Therefore, the computation cost is low. From our test, the running time of BCFI algorithm is less than 1 ms. Nevertheless, acquiring fingerprints on all floors is labor-intensive. Floor fingerprint collection with crowdsourcing is a low-cost alternative method.

D. Experimental Setup

To evaluate the performance of the BCFI algorithm, we conducted several experiments in three buildings: 1) the Institute of Computing Technology (ICT), Chinese Academy of Science, with large hollow areas from the first floor to the fourth one; 2) "xinzhongguan" (the Xin Zhongguan Mall) with small hollow interior through the bottom four floors; and 3) "bit" (the central teaching building of Beijing Institute of Technology) with corridors connecting two separate parts on the bottom three floors.

We used five Wi-Fi-enabled smartphones (Samsung Galaxy Note2/Note3/S4/S5/Ace S5830) to collect floor fingerprints. We developed an application that queried the Android Application Programming Interface (API) for the Wi-Fi fingerprints (0.5-Hz sampling rate for all smartphones). The training samples were collected at a uniform distance interval along all available paths on each floor. Each sample vector consists of the MAC addresses of all scanned APs and corresponding floor level. The signal sampling points were evenly distributed across the whole experimental area. Two neighboring sampling points were 3–5 m apart according to the specific layout condition.

The accuracy of floor identification is defined as the number of correctly identified floor over the total number of trails.

E. Results and Analysis

The performance of the BCFI algorithm is evaluated with the training samples and test samples, respectively. The test samples were collected with the same five smartphones four days after the training samples collecting time along the same paths. The leave-one-out cross-validation test was applied, and the floor identification accuracy is the average of all experiments. For comparison, we implemented Skyloc and clustering-based floor identification algorithm [15].

Three experiments were performed with the training samples: 1) single device test: using five devices collected samples to perform test, respectively; 2) mixing device test: mix five

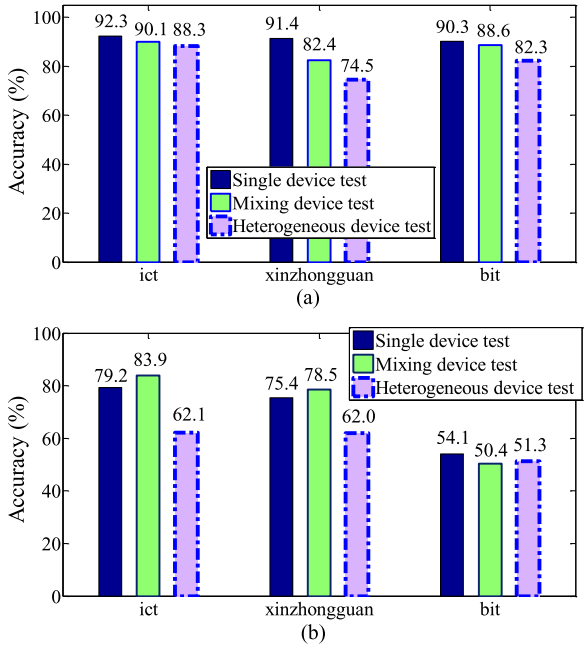

Fig. 1. Floor identification accuracy with training samples. (a) Using BCFI. (b) Using Skyloc.

TABLE I
DIFFERENT FLOOR IDENTIFICATION ACCURACY WITH TRAINING SAMPLES USING BCFI METHOD IN ICT

Floor no.	1-single device test (%)	2-mixing device test (%)	3- heterogeneous device test (%)	Hollow interior	Sample number
1	99.6	97.2	90.3	N	689
2	97.1	96.0	95.2	Y	481
3	42.5	27.1	27.0	Y	499
4	80.2	75.7	74.3	Y	531
5	99.0	98.8	98.5	N	944
6	99.3	99.4	98.0	N	863
7	98.7	98.5	95.1	N	915
8	99.6	99.6	99.6	N	797
Avg.	92.3	90.1	88.3		

devices collected samples together to evaluate; and 3) heterogeneous device test: using one device collected samples to calculate the AP distribution probability and using the other four devices collected samples to perform validation test.

As Fig. 1(a) shows, using the training samples collected from the same device (i.e., single device test), the BCFI algorithm can achieve the best accuracy (about 90%) due to more similarity between training and test samples. The heterogeneous device test shows that the accuracy degrades slightly, which confirms that the BCFI algorithm is robust. Fig. 1(b) compares the average accuracy using the three algorithms. The test results show that the probability-based floor identification (BCFI) method outperforms the shortest distance-based floor identification method (Skyloc and [15]), which reflects that the probability distribution scheme is more accurate to characterize the AP distribution on various floors within a building.

Table I lists the detailed accuracy on different floors in ICT. When the neighboring floors are partitioned with mat reinforcement concrete (e.g., the fifth floor to eighth floor), the BCFI algorithm can achieve more than 95% accuracy with the training data. This is because the wireless signal has a remarkable attenuation after propagating through a heavily partitioned concrete floor. The heavy attenuation produces different AP

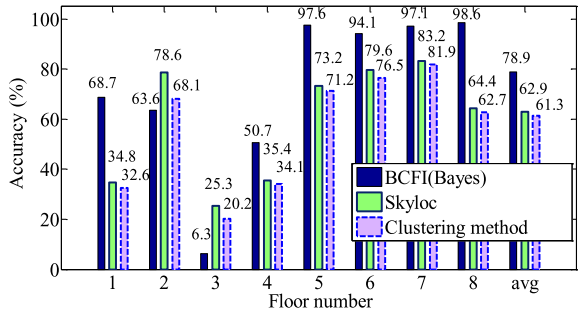

Fig. 2. Floor identification accuracy on different floors using BCFI, Skyloc, and clustering method with newly collected test samples in ICT.

sensible probabilities in each floor. But if there exists a large hollow interior through multiple floors (such as the third and fourth floors), RSSI difference between neighboring floors is rather small, which degrades the accuracy.

To evaluate the robustness of BCFI, new test samples are collected four days later in ICT. As Fig. 2 shows, the accuracy degrades remarkably on those floors with large hollow areas (from the first to fourth floor). However, on the floors partitioned with mat reinforcement concrete (such as the fifth to eighth floor), the BCFI achieves reasonable accuracy. The BCFI outperforms both the Skyloc- and clustering-based floor identification algorithms with more than 15% average accuracy.

IV. BAROMETRIC PRESSURE-BASED FLOOR IDENTIFICATION

The barometric pressure-based floor identification (hereinafter referred to as BPFI) algorithm is motivated by the fundamental that the barometric pressure drops nearly exponentially with increased altitude. Different from the Wi-Fi-based floor identification method, the BPFI algorithm can determine floor level without relying on additional infrastructure and intensive labor. Because the hollow interior within a building has no impact on barometric pressure, the BPFI algorithm can work well on all floors in various buildings with complex and irregular inner structure.

Without the need of continuously calibrating the pressure using a standard barometer deployed in the building, the BPFI algorithm introduces barometric pressure difference and quick pressure change determination, which avoids identifying floor with absolute altitude. After initializing the floor level with manual input or high-confident floor estimation with the BCFI algorithm, the BPFI algorithm employs the barometric pressure difference to determine elevation change corresponding to floor transition. To calibrate the slow accumulation of barometric pressure drift with time, we propose a novel approach to detect quick pressure change caused by a real floor transition. After discriminating the slow and quick pressure change, the BPFI algorithm only employs the obtained quick altitude change to identify the floor level.

A. Properties of Barometric Pressure

The nearly uniform exponential pressure–altitude relationship [22] is adopted by the BPFI algorithm to calculate the altitude in meters as shown in the following equation:

$$h = 44330 * (1 - (p/1013.25)^{0.19}) \quad (3)$$

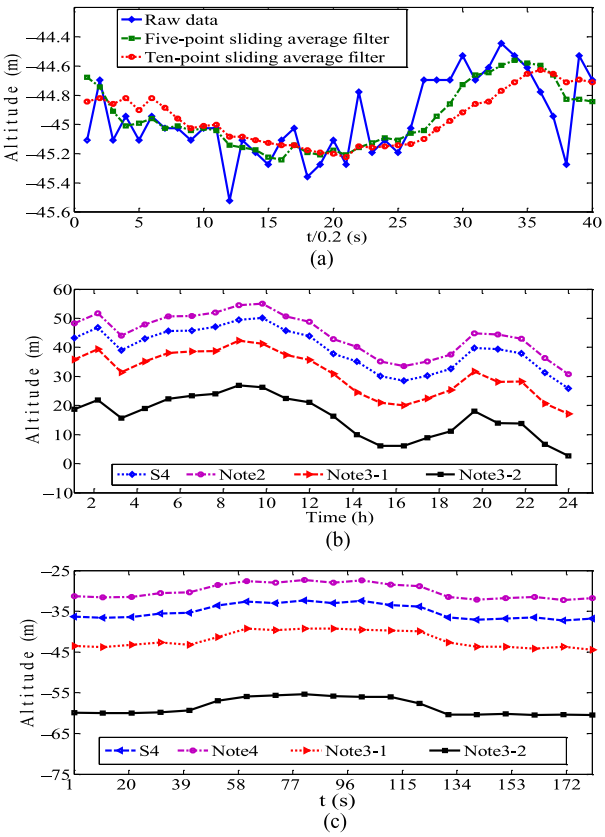

Fig. 3. Dynamic and heterogeneous properties of barometric pressure measured with barometric sensor-enabled smartphones. (a) Barometric pressure (altitude) variation with/without filtering. (b) Barometric pressure (altitude) drifts during a whole day on the same floor. (c) Barometric pressure (altitude) variations between different smartphones.

where p is the measured pressure (in hPa).

Now, the barometric sensors are widely embedded in the commodity smartphones (e.g., BMP085/180/182 [23]). The $\pm(0.12-0.2)$ hPa relative accuracy may cause $\pm(1-1.7)$ m elevation fluctuation. This sensitivity is good enough to detect the pressure change when users go upstairs or downstairs for one floor, which will produce about 0.45-hPa pressure change. By averaging several samples (most barometric sensors support 7-Hz sampling rates), the relative accuracy can be improved.

Due to the influence of wind, humidity, and small dust, the pressure measurement is dynamic. To test the sensor accuracy, we used three smartphones (i.e., one xiaomi2 and two Samsung Note 4s) to sample the barometer readings at a fixed location within a building with 5-Hz sampling rate. The red curve in Fig. 3(a) shows that the raw pressure measurements (since there exists a monotonous relationship between the altitude and the measured pressure, for being straightforward, hereafter, we use the altitude change to indicate pressure change) within 8 s are strongly influenced by noise, which causes about 1-m variation. The other two curves show the absolute pressures that are filtered by a five-point sliding average filter and a ten-point sliding average filter, respectively. They are much smoother compared to the red one after the noise of the sensor is filtered out. Therefore, the sliding average filter has a positive effect on the absolute pressure values. However, larger size of sliding window will cause more floor detection delay when a floor transition happens (refer to the experimental section). In the following tests, we employ the five-point sliding average filter to get the altitude estimation.

Compared with the small altitude variation on the same floor in tens of seconds, the long-term pressure drifts (e.g., for a whole day) can reach as large as 30 m as Fig. 3(b) shows. Even using the same type of smartphones, the altitude variation can still reach as large as 15 m. The reason for large drift is that all the barometric sensors integrated in the same type of smartphones use the same version of driver and Android software and are not calibrated, respectively. If directly using the obtained elevation to localize floor without compensation, the estimated floor level may deviate from the real floor level for nearly ten floors away. To get accurate floor estimation, this kind of slow pressure drift should be identified and mitigated.

Based on the observation that the pressure changes on the same floor or at a fixed place within a short period (e.g., 1–15 s) are rather smaller than that caused by real floor transitions, a quick pressure change identification scheme is introduced in this paper. By only using the altitude change corresponding to the quick pressure change to localize floor, the BPFI algorithm can get accurate and robust floor estimates.

As Fig. 3(c) shows, though the barometer variations between different smartphones are considerably large (5–20 m), the relative pressure drifts with time and floor transition between smartphones keep stable. It suggests that the large absolute difference between heterogeneous devices can be effectively solved by only using the relative pressure change to localize floor instead of using absolute pressure reading.

B. Distributed Self-Calibration of Barometric Pressure

To identify floor, an accurate mapping between the pressure-deriving elevation and each floor of a building needs to be constructed. To solve the pressure drift and device heterogeneity, the crowdsourcing is adopted to calibrate the barometric sensor based on the user encounter in the same elevator or bus [23], by which all smartphones need to communicate with a pressure calibration cloud center. Different from this central calibration approach, we propose a distributed self-compensation method: each smartphone builds its own elevation-floor map and compensates the slow pressure drift individually to counteract the environmental gradual change.

The pseudocode of BPFI algorithm is as shown in Fig. 4.

1) Distributed Elevation-Floor Map Construction: By associating the initial pressure with the initial manual input of floor level or by reading two-dimensional (2-D) code, each smartphone can construct its own elevation-floor map without the need of using a central pressure calibration system. After having obtained the initial reference pressure-floor map, the pressure difference is then used to estimate the elevation change instead of using the absolute altitude to localize floor.

To differentiate the pressure change with environment and floor transition, we divide the elevation $h(t)$ deriving from the pressure–altitude model [as (3) shows] into two parts

$$h(t) = h_{\text{envi}}(t) + h_{\text{floor}}(t) \tag{4}$$

(1) System initialization
(2) Obtain the initial floor level and corresponding barometric pressure
(3) Construct the altitude-floor map
(4) *count*=0; //for slow changes
(5) While (true)
(6) If ($\Delta h(t) > \varepsilon$) //quickly changes
(7) $h_{floor}(t)=h_{floor}(t\text{-}1)+\Delta h(t)$; //update altitude
(8) $Floor(t)=get\_floor(h_{floor})$; // update floor with the altitude-floor map
(9) $Count=0$;//clean slow changes
(10) else *count*++; //slow changes
(11) End if
(12) If (*count*>*n*) //successive altitude changes are less than threshold
(13) $h_{floor}(t)= get\_height(Floor)$; // current floor altitude in the altitude-floor map
(14) End if
(15) End while

Fig. 4. Pseudocode of BPFI algorithm.

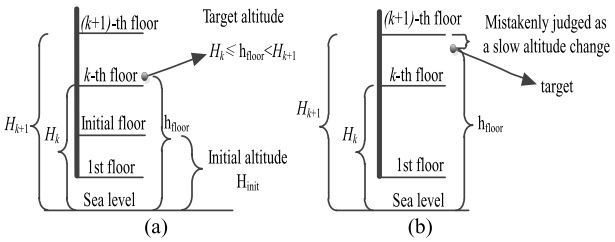

Fig. 5. Individual altitude–floor map for individual smartphone.

where $h_{\text{envi}}(t)$ is the slow change altitude part caused by environmental factors, $h_{\text{floor}}(t)$ is the quick change part caused by floor transitions. Only the quick change part $h_{\text{floor}}(t)$ is used for floor estimation, while the slow change part $h_{\text{envi}}(t)$ is used for compensating the gradual altitude change due to weather variation. The pressure change pattern can be accurately identified with our proposed threshold-based scheme (for more details, see the next section)

At the initial time ($t = 0$), we assume that

$$h_{\text{envi}}(0) = 0, \quad h_{\text{floor}}(0) = H_{\text{init}} \tag{5}$$

where H_{init} is the initial floor altitude calculated from the initial measured pressure $P_{\text{init}}(0)$.

After associating the manual input floor level L_{init} with the initial floor altitude H_{init}, combined with the prior floor height of a building $\{d_1, d_2, \ldots, d_n\}$ (d_i is the ith floor height, $1 \le i \le n$, n is the total floor number of the building), each smartphone constructs its individual altitude-floor map as follows:

If $((H_k+H_{k-1})/2 \le h_{\text{floor}} < (H_k+H_{k+1})/2)$, then $h_{\text{floor}} \Leftrightarrow H_k$ (target is judged to be on the kth floor), where $\begin{cases} H_1 = H_{\text{init}} - (\sum_{i=1}^{L_{\text{init}}-1} d_i) \\ H_k = H_1 + \sum_{i=1}^{k-1} d_i, \ 2 \le k \le n \end{cases}$, H_k is the altitude of the kth floor, as shown in Fig. 5(a).

Due to the device heterogeneity, the initial pressure measured by each smartphone is different on the same floor, so the attitude-floor map built by individual smartphone is different. However, the pressure differences corresponding to the same floor transition measured by different devices are consistent. Once each smartphone has constructed its own altitude-floor map, it can determine floor locally only with the identified quick altitude change (i.e., quick pressure change).

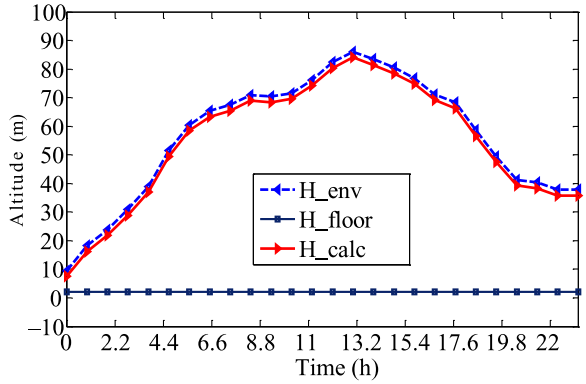

Fig. 6. Performance of slow pressure drift self-calibration in 24 h in a fixed place.

2) Slow Pressure Drift Self-Calibration: In a fixed place or on a same floor, though the real altitude keeps unchanged, the altitude change deriving from pressure drift may accumulate to several floors away in a couple of hours due to environmental effects. To compensate this gradual pressure change, we proposed a threshold-based scheme to detect the pressure change pattern based on the observation that the environmental pressure change within a determination period is much smaller than that caused by a floor transition.

The self-calibration processing is as follows. After initialization, the device starts to measure the environmental pressure periodically and calculates the altitude change $\Delta h(t)$ within each floor-identification period Δt using the observed pressure change. Corresponding to the (4), the total altitude change $\Delta h(t)$ comprises of two parts

$$\Delta h(t) = \Delta h_{\text{envi}}(t) + \Delta h_{\text{floor}}(t). \tag{6}$$

The first part is the gradual altitude drift $\Delta h_{\text{envi}}(t)$ due to environmental pressure change, and the second is the quick altitude change $\Delta h_{\text{floor}}(t)$ produced by a real floor transition.

If the pressure change $\Delta h(t)$ within the current floor identification period $[t\text{-}\Delta t, t]$ is judged to be slow pressure drift type, it is added to the $h_{\text{envi}}(t)$ and excluded from the floor transition processing as follows:

$$\text{If } \Delta h\,(t) < \Delta h_{\text{th}}, \text{ then } \begin{cases} h_{\text{envi}}(t) = h_{\text{envi}}(t-\Delta t) + \Delta h(t) \\ h_{\text{floor}}(t) = h_{\text{floor}}(t-\Delta t). \end{cases}$$

Using this slow pressure drift self-calibration method, the BPFI can effectively eliminate pressure drift accumulation. As Fig. 6 demonstrates, when a user stays on a floor for a whole day (e.g., 24 h), while the slow pressure drifts reach as large as 80 m, the identified quick pressure change and floor-level identification remain unchanged.

3) Floor Update With Quick Pressure Change: If the pressure change $\Delta h(t)$ within the current floor identification period $[t\text{-}\Delta t, t]$ is judged to be a quick altitude change type, it is added to the $h_{\text{floor}}(t)$, i.e.,

$$\text{If } \Delta h(t) \ge \Delta h_{\text{th}}, \text{ then } \begin{cases} h_{\text{floor}}(t) = h_{\text{floor}}(t-\Delta t) + \Delta h(t) \\ h_{\text{envi}}(t) = h_{\text{envi}}(t-\Delta t). \end{cases}$$

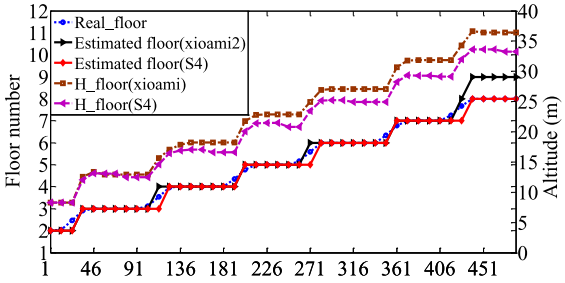

Fig. 7. Small floor transition errors accumulate with the number of floor transition with and without calibration.

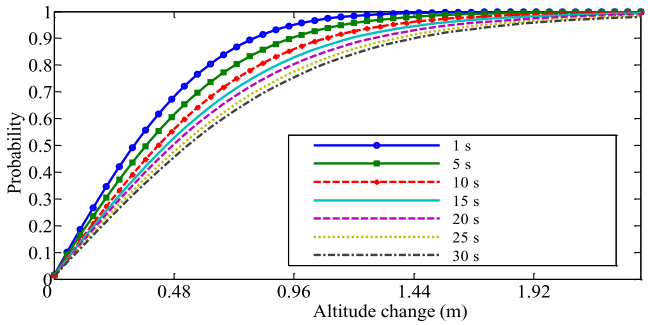

Fig. 8. Altitude change distribution with different sampling periods.

After having obtained a new $h_{\text{floor}}(t)$, the floor level is updated using the previously built attitude-floor map.

4) Altitude Compensation for Floor Transition: When a real floor transition happens, the pressure may not be sampled exactly on the floor level, as Fig. 5(b) shows. The previous measurement is taken when the user is located below the kth floor by less than 1.5 m, and at the next pressure sampling instant, the user has been on the kth floor for several seconds. Because the altitude change is less than the identification threshold, the latest pressure change is mistakenly judged as the slow pressure change pattern and is added to the environmental altitude change $\Delta h_{\text{envi}}(t)$.

To compensate this small altitude offset of floor transition, we use the latest identified floor altitude in the altitude-floor map to directly replace the floor altitude calculated from the quick pressure change after having detected several successive slow pressure changes (i.e., the pressure measurement becomes stable). As Fig. 7 shows, this small altitude offset can be effectively calibrated by using this compensation scheme.

C. Optimal Floor Identification Period Selection

To accurately differentiate the slow altitude change and quick altitude change, an optimal floor identification period should be selected. If the identification period is set too short, the pressure difference between two successive measurements for a floor transition is also small that is indistinguishable from the slow pressure change or fluctuation. If the identification period is set too long, the determination delay is large.

The optimal selection of floor identification period considers the following rules.

1) The absolute pressure change caused by a real floor transition within one identification period should be greater than the absolute pressure drift due to environmental influence within one floor identification period.
2) The floor determination delay should be short.

When users take elevators, the altitude will change dozens of meters within tens of seconds. When users climb upstairs slowly, the pressure changes rather gradually. Because there is no theoretical solution for the optimal collection period selection, we obtain the optimal floor identification period with empirical method.

Fig. 8 demonstrates the altitude change distribution with different floor identification periods.

Fig. 9 shows the altitude changes with the increase in identification periods. To accurately discriminate the minimum quick altitude change caused by slow floor transition and the gradual altitude change due to environmental factors and sensor noise with 95.44% confidence (2σ), the identification period should be larger than 15 s. If we want to further improve the confidence to detect larger gradual altitude change caused by environmental factors, the identification period should be further increased, which will result in larger delay and decrease in relative accuracy (i.e., the small quick altitude change cannot be determined using large threshold and cannot be differentiated from the gradual altitude change). To balance the floor identification delay and accuracy, the optimal identification period is selected to 15 s in the following experiments.

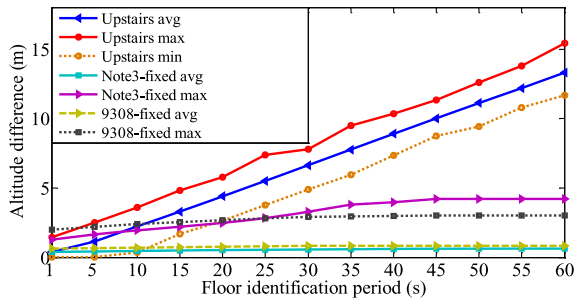

Fig. 9. Selection of optimal floor identification period.

D. Experimental Results and Analysis

1) Experimental Setup: For the convenience of floor computing, all pressure measurements (5-Hz sampling rate) are first converted into altitude, and then filtered with a five-point moving averaging filter to eliminate noise. All the filtered altitude data are added to a First In First Out (FIFO) queue. Once a new altitude is obtained, subtract it with the head of the altitude queue to get the latest altitude change. To balance the pressure measurement accuracy and floor determination delay, we set the queue length to 15, i.e., altitude change within 15 s as a comparison unit.

Among various floor transitions, climbing upstairs is the slowest quick altitude change, which determines the lower bound of quick pressure change. The pressure change pattern identification should be able to differentiate the slow pressure change caused by environment with this pressure change due to going upstairs. By real test in our ICT building, we get the average speed of altitude changing with about 0.13 m/s when going upstairs. Accounting for the 15-s optimal floor identification

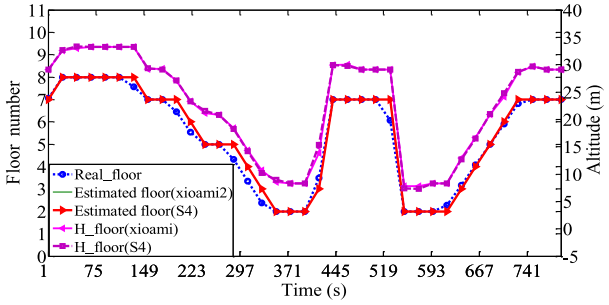

Fig. 10. Floor estimation results using BPFI in short-term periods.

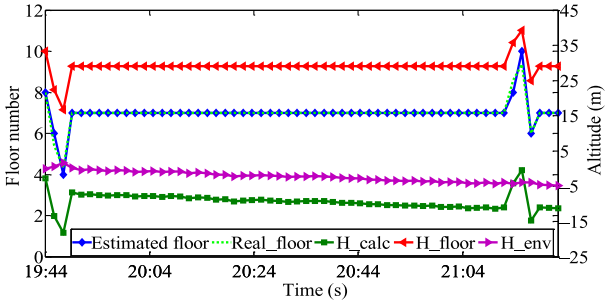

Fig. 12. Floor estimation using BPFI algorithm in long-term periods.

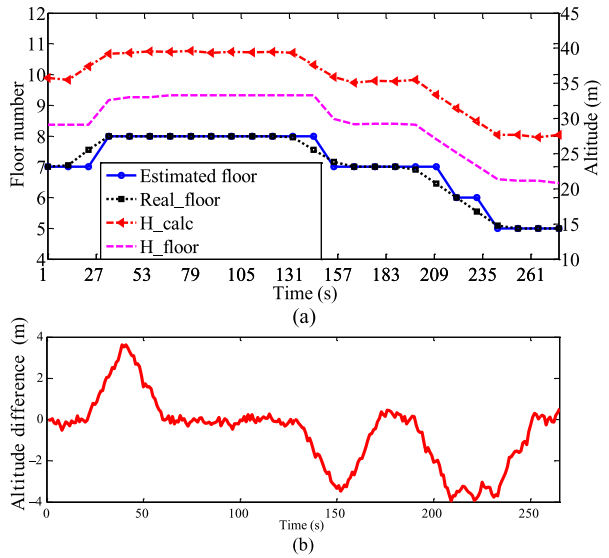

Fig. 11. Detailed altitude changes under real floor transitions. (a) Altitude changes under real floor transition. (b) Altitude difference under real floor transition corresponding to (a).

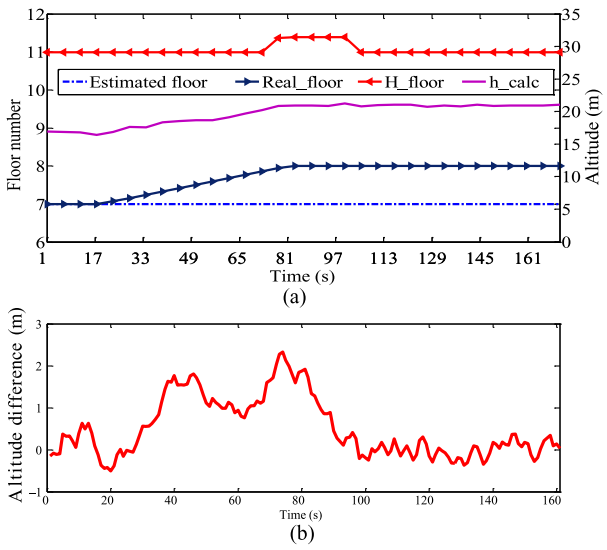

Fig. 13. Floor identification failure under very slow floor transition with BPFI. (a) Floor identification failure under very slow floor transition. (b) Small altitude difference under very slow floor transition.

period, the pressure change threshold is set to 1.7 m in the following experiments.

2) Floor Identification Performance: After initializing the floor with manual input floor number 7, we started to evaluate the BPFI algorithm by first going upstairs to the eighth floor in the east part of our ICT building with two smartphones (Xiaomi 2s and Samsung S4) being held together, then went downstairs from the eighth floor to the first floor, next crossed the ground hall to the west part of ICT, then took the west elevator directly from the first floor to the seventh, walked through the corridor to the east elevator and took the elevator down to the first floor, at last went upstairs from the first floor to the seventh floor again. As Fig. 10 shows, though the initial and online altitude measurements by two devices are different, the floor estimations are all correct, which confirms the robustness of the proposed BPFI to device heterogeneity.

Fig. 11 demonstrates the altitude change in more details. When a user stays on a floor, the quick change part $h_{\text{floor}}(t)$ remains constant. While the whole altitude $h(t)$ drifts with time, all the altitude changes $\Delta h(t)$ (pressure change) within a floor identification period are less than the pressure change threshold Δh_{th}, so the floor level keeps unchanged. When the user starts to go upstairs or downstairs, both the whole altitude $h(t)$ and the quick change part $h_{\text{floor}}(t)$ change monotonously, and the altitude change within a floor identification period exceeds the altitude change threshold, so the floor level updates accordingly. From the plot, we can see that there is about ten seconds of floor identification delay because of the influence of filtering processing and quick altitude change determination threshold. There are three times of small altitude compensation operation shown in Fig. 11 after the user reaches the destination floor level and the pressure measurements become stable.

Fig. 12 shows that the BPFI algorithm can still achieve accurate floor determination results with 1 h and 40 min interval between two successive floor transitions. It confirms that the BPFI is robust to the slow pressure change caused by environment. However, when a very slow floor transition happens, as Fig. 13 denotes, the quick altitude change within a floor identification period is less than the predefined threshold, so the BPFI cannot detect the floor transition.

V. Hybrid Floor Identification Algorithm

As the above section describes, either of the BCFI and BPFI algorithm has pros and cons. The floor identification with BCFI algorithm is consistent with the ground-truth floor only on the heavily partitioned floors with mat reinforcement concrete from neighboring floors. On the floors with hollow interior, especially in the areas near the hollow edge, the estimated floor using the BCFI often deviates by 2–3 floors away from the truth.

```
(1) While (true)
(2) Collecting Wi-Fi fingerprints and localizing floor level using BCFI
(3) If BCFI succeeds and posterior probability>0.6
(4)   Initial BPFI algorithm with the floor identification result
(5)     Break
(6) End if
(7) End while
(8) While (true)
(9) Collecting Wi-Fi fingerprints and localizing floor level using BCFI
(10) If BCFI succeeds and posterior probability >0.6
(11)       Updating BPFI with floor identification result
(12)  End if
(13) Collecting pressure and localizing floor level using BPFI
(14) End while
```

Fig. 14. Pseudocode of HYFI algorithm.

For the BPFI algorithm, it can accurately determine floor level in complex and irregular indoor environments if an accurate initial floor level is given with manual effort. However, if small quick altitude changes have not been detected and the altitude compensation for floor transition does not take effect (e.g., a user climbs upstairs for several steps and rest for tens of seconds, and then goes up), which will produce erroneous floor identification result.

A. Hybrid Scheme of HYFI Algorithm

To eliminate manual input and influence of mistaken floor determination by slow floor transition, we adopted a novel hybrid floor identification scheme (hereinafter referred to as HYFI). The BPFI algorithm is initialized and calibrated opportunistically once getting a high-confidence floor estimation on the floors that are heavily partitioned with mat reinforcement concrete from neighboring floors with the BCFI algorithm. After initialization or calibration, the HYFI uses the BPFI algorithm to localize the floor until receiving another high confident floor estimation obtained with the BCFI algorithm.

The pseudocode of HYFI algorithm is as shown in Fig. 14.

In detail, a floor-level estimation is assumed to be a high-confident floor estimation if the following two items are met:

$$\text{if} \begin{cases} P_{\max}\left(l|o\right)\left(t\right) \geq \alpha \\ |\Delta h(t)| \leq \Delta h_{th} \end{cases}$$

where $P_{\max}(l|o)(t)$ is the largest posterior probability, parameter α is used to evaluate the confidence of floor identification, and its optimal value is selected by trials. To eliminate the uncertainty when going upstairs or downstairs, the BCFI algorithm is not used for calibration, i.e., only when the user reaches the target floor and the pressure observations get stable, the floor identification result with the BCFI can be used to calibrate the BPFI. On the floors that are heavily partitioned with mat reinforcement concrete from neighboring floors, the largest posterior probability is remarkably larger than that on the floors with hollow interiors through adjacent floors.

By introducing calibration with high confident floor estimation obtained with the BCFI algorithm, the HYFI can identify floors accurately in various buildings, especially in the floors with complex and irregular hollow interior structure.

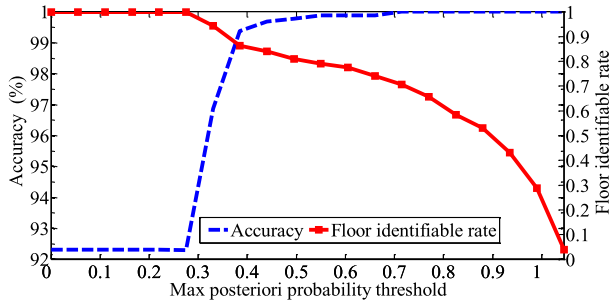

Fig. 15. Influence of posterior probability threshold.

B. Experimental Results and Analysis

In the following experiments, the "accuracy" is defined as the accurate percentage with the selected posterior probability greater than the predefined threshold to determine floor level. The "rate" represents the ratio of number of accurate floor identification with posterior probability greater than threshold to the total number of floor identification test times, i.e., floor identifiable rate. Because there is no barometric sensor integrated in S5830 and Samsung Galaxy S5, in the following tests, we use Galaxy Note 2/3, Samsung Galaxy S4 to evaluate the performance in ICT building.

1) Influence of Threshold Parameter α: Fig. 15 illustrates the floor identification accuracy improvement with the increase in posterior probability threshold parameter α.

When we use the maximum posterior probability criteria to determine floor level for each Wi-Fi observation, the average floor identification accuracy is about 92%. When adopting the proposed high-confident floor identification criteria, i.e., only choosing those maximum posterior probabilities which are larger than the predefined threshold to perform floor determination, the floor identification accuracy increases rapidly to nearly 100%, while the floor identifiable rate decreases quickly. To achieve the desired tradeoff between accuracy and identifiable rate, in the following experiments, the probability threshold is set to 0.7.

2) Influence of Threshold Limit on BCFI: The BCFI with different threshold is evaluated in ICT buildings, as Table II shows. Only using the posterior probabilities larger than the predefined threshold (0.7) to determine floor, we can obtain more than 99.0% accuracy. However, the floor identifiable rate decreases with the increase in posterior probability threshold. Especially on the floors with hollow areas, the floor identifiable rate is rather low because of Wi-Fi fingerprinting similarity between adjacent floors.

3) Performance of HYFI: To better evaluate the performance of HYFI algorithm, we collect test samples with the same smartphones at different time in the ICT building. We use these newly collected test samples to perform floor identification instead of using training samples. The real floor transition trajectory is shown in Fig. 16. From the beginning to the 18th min, the user went upstairs and downstairs at normal speed. After that, the user went upstairs and downstairs at a very slow speed, which is used to evaluate the robustness of the HYFI under slow pressure change.

TABLE II
FLOOR IDENTIFICATION ACCURACY WITH TRAINING SAMPLES USING BCFI WITH THRESHOLD LIMIT IN ICT BUILDING

Floor no.	1-single device test		2-mixing device test		3-heterogeneous device test	
	Accuracy (%)	Rate (%)	Accuracy (%)	Rate (%)	Accuracy (%)	Rate (%)
1	100.0	35.3	100.0	28.1	98.6	38.1
2	100.0	73.2	100.0	69.7	100.0	71.1
3	94.1	3.2	0.0	0.0	16.8	0.9
4	99.5	40.5	96.4	24.8	95.8	34.1
5	99.9	97.5	99.4	94.2	99.8	93.1
6	100.0	94.4	100.0	81.0	99.6	85.6
7	100.0	90.4	99.3	81.6	96.9	84.9
8	100.0	99.6	99.4	98.1	99.7	98.6
Avg.	99.9	73.1	99.5	66.0	98.4	69.4

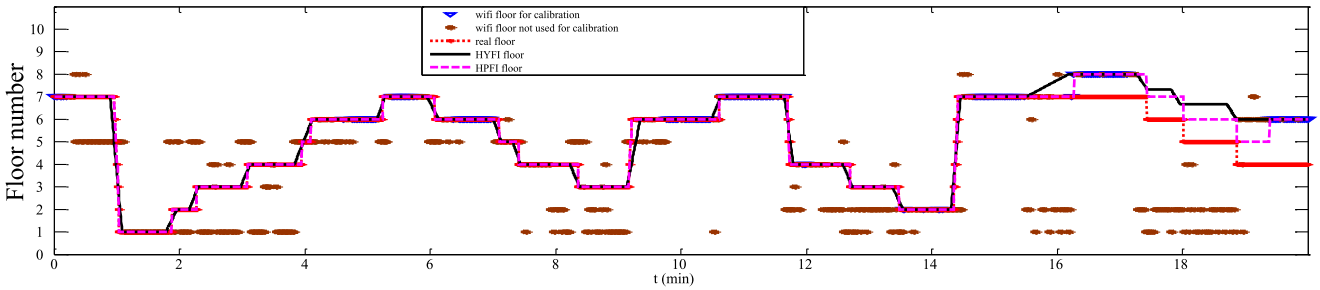

Fig. 16. Floor identification comparison using BCFI/BPFI/HYFI with regular and slow speed going upstairs and downstairs.

TABLE III
CALIBRATION OF BPFI ON DIFFERENT FLOORS USING HIGH CONFIDENT BCFI RESULT IN ICT BUILDING

Floor no.	Wifi sample number	Wifi correct number	Wifi number used for calibration	Wifi number used for correct calibration	BCFI correct rate (%)	Correct rate used for calibration (%)	BPFI sample number	BPFI correct number	BPFI correct rate (%)	HYFI sample number	HYFI correct number	HYFI correct rate (%)
1	33	32	0	0	97.0	0/0	62	62	100	94	94	100
2	46	35	6	6	76.1	100	88	88	100	134	134	100
3	98	4	0	0	4.1	0/0	187	187	100	285	285	100
4	109	43	3	3	43.4	100	205	205	100	314	314	100
5	9	9	9	9	100	100	17	17	100	26	26	100
6	183	151	91	91	82.5	100	390	274	70.3	573	502	87.6
7	164	131	98	98	79.9	100	336	336	100	500	500	100
8	37	35	24	24	94.6	100	112	0	0	149	138	92.6
Sum	679	440	231	231	64.8	100	1397	1169	83.7	2075	1993	96.1

From Fig. 15, we can see that the BPFI algorithm is accurately initialized and frequently calibrated by the BCFI algorithm on the floors partitioned with heavy concrete floor slabs (the sixth, seventh, and eighth floor) through the whole experimental period in spite of moving speed. By the accurate initialization and frequent calibration of BPFI, the HYFI algorithm identifies floor level with 96.1% accuracy, as Table III denotes. The detailed calibration number of BPFI on different floors using high-confident BCFI result is also shown in the table. From the fifth and eighth floors, because adjacent floors are partitioned with heavy-concrete floor slabs, about half floor identification results are high confident and used to calibrate the BPFI algorithm. Nevertheless, from the first to fourth floor, the BPFI algorithm is calibrated for few times. That is because there is large hollow interior through these four floors and the floor identification confidence with the BCFI algorithm on these floors is rather low.

As a comparison, when there is only accurate initialization for the BPFI algorithm but without subsequent calibration by the BCFI algorithm, the BPFI fails giving any right floor identification after the 18th min once a slow-going upstairs or pausing happens, which corresponds to a slow pressure change. The corresponding pressure change within an identification period is less than the pressure quick change threshold and then one floor-level difference is produced by the BPFI. From the 18th min and 30th s, we went downstairs from the eighth floor to the sixth floor, and we paused two times on the stairs. The BPFI algorithm fails again detecting the floor transition and produces wrong floor determination results as large as two floors away from the actual floor level. However, after we reached the

sixth floor for 20 s, the BPFI is calibrated by the BCFI algorithm and the HYFI gives the accurate floor identification again, which demonstrates that the HYFI algorithm can eliminate the floor identification failure propagation by opportunistic calibration with the BCFI algorithm and is robust to different moving speed.

VI. Discussion and Conclusion

A. Discussion on Use Cases

Obviously in commercial buildings, high-accuracy floor identification is important for such as location-based promotion and advertisement in shopping malls, navigation services in train stations and airports, tracking and navigation of patients, and equipment in hospitals. For emergency services like first aid, rescue, firefighting, and public security, it is also crucial to improve efficiency of actions in complicated multistory buildings—time is life!

In industrial buildings and facilities, we have also seen many promising use cases for the proposed technologies for tracking and navigating vehicles, robots, and personnel [24]. For example, in construction industry, real-time location and floor number of workers, lifts and cranes can be used to improve the safety of workers and efficiency of task coordination [5]. Real-time localization and floor identification is one of the enabling technologies for realizing man-less inspection of facilities by autonomous robots in dangerous or safety-critical industrial sites [25]. In modern mining industry, the underground tunnels are more and more equipped with wireless communication infrastructure like Wi-Fi, which makes it possible to realize cost-effective tracking of miners and equipment based on the proposed solution [3], [26]. Moreover, in the remote collaboration service where field operators or commissioners get real-time support from remote experts through bidirectional audio and video interaction, accurate location and floor number can help the remote experts know where the field operators exactly are, which can significantly save time and reduce the probability of miss-instructions.

B. Conclusion

In this paper, we have demonstrated the possibility of floor identification combined with the Wi-Fi AP distribution and barometric pressure information in the complex multistory buildings. Through the selection of the floor estimation with high confidence opportunistically obtained with Wi-Fi distribution in well-partitioned zones, to initialize and calibrate barometric pressure-based floor identification, the proposed hybrid floor identification approach outperforms both Wi-Fi-based floor identification and barometric pressure-based floor identification. Furthermore, this approach can identify floors accurately in irregular multistory buildings, especially in the floors with complex hollow interior structure.

Our future work will incorporate this floor identification approach into the Wi-Fi fingerprinting localization system to speed up the localization progress as well as extending the capability of indoor positioning system to multistory buildings.

References

[1] J. N. Bakambu, V. Polotski, and P. Cohen, "Heading-aided odometry and range-data integration for positioning of autonomous mining vehicles," in *Proc. Int. Conf. Control Appl.*, Anchorage, AK, USA, Sep. 2000, pp. 279–284.

[2] E. DiGiampaolo and F. Martinelli, "Mobile robot localization using the phase of passive UHF RFID signals," *IEEE Trans. Ind. Electron.*, vol. 61, no. 1, pp. 365–376, Feb. 2013.

[3] B. Silva, Z. Pang, J. Åkerberg, J. Neander, and G. Hancke, "Positioning infrastructure for industrial automation systems based on UWB wireless communication," in *Proc. 40th Int. Conf. Ind. Electron. Soc. (IECON'14)*, Dalla, TX, USA, Oct. 2014, pp. 3919–3925.

[4] F. Duvallet and A. D. Tews, "Wi-Fi position estimation in industrial environments using Gaussian processes," in *Proc. IEEE/RSJ Int. Conf. Intell. Robots Syst.*, Nice, France, Sep. 22–26, 2008, pp. 2216–2221.

[5] T. Cheng and J. Teizer, "Real-time resource location data collection and visualization technology for construction safety and activity monitoring applications," *Autom. Constr.*, vol. 34, pp. 3–15, 2013.

[6] U. Rüppel, K. M. Stübbe, and U. Zwinger, "Indoor navigation integration platform for firefighting purposes," in *Proc. 1st Int. Conf. Indoor Positioning Indoor Navigat. (IPIN'10)*, Zürich, Switzerland, Sep. 2010, pp. 1–6.

[7] H. Liu, H. Darabi, P. Banerjee, and L. Jing, "Survey of wireless indoor positioning techniques and systems," *IEEE Trans. Syst. Man Cybern. C, Appl. Rev.*, vol. 37, no. 6, pp. 1067–1080, Nov. 2007.

[8] S. Lee, B. Kim, H. Kim, R. Ha, and H. Cha, "Inertial sensor-based indoor pedestrian localization with minimum 802.15.4a configuration," *IEEE Trans. Ind. Informat.*, vol. 7, no. 3, pp. 455–466, Aug. 2011.

[9] J. Park and J. Lee, "A beacon color code scheduling for the localization of multiple robots," *IEEE Trans. Ind. Informat.*, vol. 7, no. 3, pp. 467–475, Aug. 2011.

[10] J. Rodriguez-Araujo, J. J. Rodriguez-Andina, J. Farina, and M. Y. Chow, "Field-programmable system-on-chip for localization of UGVs in an indoor iSpace," *IEEE Trans. Ind. Informat.*, vol. 10, no. 2, pp. 1033–1043, May 2014.

[11] U. Larsson, J. Forsberg, and A. Wernersson, "Mobile robot localization: Integrating measurements from a time-of-flight laser," *IEEE Trans. Ind. Electron.*, vol. 43, no. 3, pp. 422–431, Jun. 1996.

[12] J. A. Hesch, D. G. Kottas, S. L. Bowman, and S. I. Roumeliotis, "Consistency analysis and improvement of vision-aided inertial navigation," *IEEE Trans. Robot.*, vol. 30, no. 1, pp. 158–176, Feb. 2014.

[13] A. Varshavsky, A. LaMarca, J. Hightower, and E. de Lara, "The Skyloc floor localization system," in *Proc. 5th Annu. IEEE Int. Conf. Pervasive Comput. Commun. (PerCom'07)*, 2007, pp. 125–134.

[14] F. Alsehly, Z. Sevak, and T. Arslan, "Indoor positioning with floor determination in multi-story buildings," in *Proc. Int. Conf. Indoor Positioning Indoor Navigat. (IPIN'11)*, Guimarães, Portugal, Sep. 21–23, 2011, pp. 1–7.

[15] Z. L. Deng, W. J. Wang, and L. M. Xu, "A k-means based method to identify floor in WLAN indoor positioning system," *Software*, vol. 12, pp. 114–117, 2012.

[16] K. Muralidharan, A. J. Khan, A. Misra, R. K. Balan, and S. Agarwa, "Barometric phone sensors—More hype than hope," in *Proc. ACM HotMobile*, Santa Barbara, CA, USA, Feb. 26–27, 2014, pp. 1–6.

[17] K. Q. Liu, Y. J. Wang, and J. Wang, "Differential barometric altimetry assists floor identification in WLAN location fingerprinting study," in *Principle and Application Progress in Location-Based Services*. New York, NY, USA: Springer, 2014, pp. 21–29.

[18] H. Ye *et al.*, "FTrack: Infrastructure-free floor localization via mobile phone sensing," in *Proc. 10th Int. Conf. Pervasive Comput. Commun. (PerCom'12)*, Mar. 2012, pp. 2–10.

[19] H. Yei, T. Gu, X. Tao, and J. Lu, "B-Loc: Scalable floor localization using barometer on smartphone," in *Proc. IEEE Int. Conf. Mobile Ad Hoc Sensor Syst. (MASS'14)*, Philadelphia, PA, USA, Oct. 28–30, 2014, pp. 127–135.

[20] A. S. Al-Ahmadi, A. I. Omer, M. R. Kamarudin, and T. A. Rahman, "Multi-floor indoor positioning system using Bayesian graphical models," *Prog. Electromagn. Res. B*, vol. 25, pp. 241–259, 2010.

[21] M. Youssef and A. Agrawala, "The Horus WLAN location determination system," in *Proc. 3th Int. Conf. Mobile Syst. Appl. Serv. (MobiSys'05)*, Seattle, WA, USA, Jun. 2005, pp. 205–218.

[22] M. N. Berberan-Santos, E. N. Bodunov, and L. Pogliani, "On the barometric formula," *Amer. J. Phys.*, vol. 65, no. 5, p. 404, 1997.

[23] H. B. Ye, T. Gu, X. P. Tao, and J. Lu, "SBC: Scalable smartphone barometer calibration through crowdsourcing," in *Proc. Int. Conf. Mobile Ubiquitous Syst. Comput. Netw. Serv. (Mobiquitous)*, London, Great Britain, Dec. 2–5, 2014, pp. 60–69.

[24] W. Kurschl, W. Gottesheim, S. Mitsch, and W. Beer, "Towards a unified location tracking system for heterogeneous industrial environments," in *Proc. IEEE Int. Conf. Ind. Informat. (INDIN'08)*, Daejeon, Korea, Jul. 13–16, 2008, pp. 1267–1272.
[25] S. Nazlibilek, "Autonomous navigation of robotic units in mobile sensor network," *Measurement*, vol. 45, pp. 938–949, 2012.
[26] L. Thrybom, M. Gidlund, and J. Neander, "Key requirements for successful deployment of positioning applications in industrial automation," in *Proc. 4th Int. Conf. Indoor Positioning Indoor Navigat. (IPIN'13)*, Montbeliard, France, Oct. 28–31, 2013, pp. 213–216.

Fang Zhao received the B.S. degree in computer science and technology from the Huazhong University of Science and Technology, Wuhan, China, in 1990, and the M.S. and Ph.D. degrees in computer science from the Beijing University of Posts and Telecommunications, Beijing, China, in 2004 and 2009, respectively.

She is currently a Professor with the School of Software Engineering, Beijing University of Posts and Telecommunications. Her research interests include mobile computing, location-based services, and computer network.

Haiyong Luo (M'08) received the B.S. degree in electronics and information engineering from the Huazhong University of Science and Technology, Wuhan, China, in 1989; the M.S. degree in information and communication engineering from the Beijing University of Posts and Telecommunications, Beijing, China, in 2002; and the Ph.D. degree in computer science from the University of Chinese Academy of Sciences, Beijing, in 2008.

He is currently an Associate Professor with the Institute of Computing Technology, Chinese Academy of Sciences. His research interests include pervasive computing, mobile computing, and Internet of Things.

Xuqiang Zhao received the B.S. degree in computer science and technology from the Beijing Institute of Technology, Beijing, China, in 2014, where and is pursuing the Master's degree in computer science and technology.

His research interests include the information security of smart phone, with a focus on data storage security.

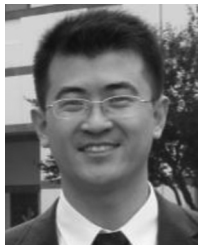

Zhibo Pang (M'13–SM'15) received the B.S. degree in electronic engineering from Zhejiang University, Hangzhou, China, in 2002; the MBA degree in innovation and growth from the University of Turku, Turku, Finland, in 2012; and the Ph.D. degree in electronic and computer systems from the Royal Institute of Technology, Stockholm, Sweden, in 2013.

He is currently a Senior Scientist and Project Manager with ABB Corporate Research, Västerås, Sweden. His research interests include the Internet-of-Things, industrial communication, automation networks, multicore system-on-chip, and network-on-chip.

Hyuncheol Park received the B.S. and M.S. degrees in electronic engineering from Yonsei University, Seoul, Korea, in 2007 and 2009, respectively.

He has been a Senior Engineer with Samsung Electronics, Suwon, South Korea, since 2009. His research interests include biosignal processing, human–computer interaction, context-aware computing, low-power system, and location-based technologies and services.